Malaysian Journal of Mathematical Sciences 15(1): 147–160 (2021)

MALAYSIAN JOURNAL OF MATHEMATICAL SCIENCES

Journal homepage: http://einspem.upm.edu.my/journal

Micropolar Fluid Flow in Tapering Stenosed Arteries having Permeable Walls

Prasad, K. M. [1] and Yasa, P. R. [*2]

[1] *Department of Mathematics, School of Science, GITAM University, India*
[2] *Department of Basic Sciences and Humanities, B. V. Raju Institute of Technology, India*

E-mail: prabhakerreddy.yasa@gmail.com
[*] *Corresponding author*

Received: 25 July 2020
Accepted: 26 December 2020

ABSTRACT

The impact of slip on micropolar fluid through inclined tapering stenosed artery having permeable walls is studied. To compute the phenomena of Nanoparticle and Temperature profiles, Homotopy Perturbation Method (HPM) is considered. The analysis with respect to different flow parameters on flow impedance ($\bar{\lambda}$) and shear stress (τ_h) are anticipated by deriving equations for the flow characteristics and solutions are obtained. The stream lines in diverging region (ξ>0), Non-tapered region (ξ=0) and converging region (ξ<0) are drawn to view flow patterns for different values of the fluid flow parameters.

Keywords: Tapered artery, stenosis, micropolar fluid, permeability constant, shape parameter.

1. Introduction

In human body, blood has a significant and magnanimous role to be considered for multi-part blending. Experimental and Theoretical investigations of the circulatory problems reveal that inflicting deaths in majority of instances have been the subject of scientific research from past years. Stenosis is more popularly observed valvular cardiovascular diseases in the developed and developing nations of the world. In recent days, many individuals are experiencing cardiovascular diseases like Stenosis, which causes demise of individuals. Vascular fluid dynamics study plays a significant job over the improvement of vascular stenosis. It is one of the human body's most serious heart disease that results to cardiovascular system failure. Depending on the extent of the stenosis the fluid circulation is disrupted.

Prasad et al. (2010) and Prasad et al. (2015) discussed the peristaltic transport of micropolar and nanofluid in an inclined tube with effect on heat and mass transport. Fluids with micro structure having referred to micropolar fluids, belonging to the category of fluids with non-symmetrical stress tensor referred to as a polar fluid.

Eringen (1966) presented the possibility of basic microfluids to represent concentrated suspensions of impartially light deformable substances in a viscous fluid. These models of fluid flow have numerous applications in engineering and physiological problems. The impact of post-stenotic effects treating blood as Bingham plastic fluid, dilatation and multiple stenosis through an artery is explored by Kumar and Diwakar (2013). The mathematical modelling of micropolar blood flow under the body acceleration and magnetic field in a stenosed artery is studied by Haghighi et al. (2019).

Many of the proposed theoretical facts and analysis on the blood flow were meticulously guessed that blood in the human body has a behaviour of Newtonian or non-Newtonian fluid. Researchers like Prasad and Yasa (2020), studied the flow of micropolar fluid with nanoparticles having non-uniform cross section with multiple stenosis. A blood flow model of micropolar fluid through a tapered artery with a single stenosis is studied by Abdullah and Amin (2010).

Many of the proposed theoretical prototypes that are examined inside the blood flow of circular channel that has a single stenosis. This Newtonian blood behavior argument is worthy for high shear rate stream. However, blood exhibits non-Newtonian properties in many cases. [Shukla et al. (1980), Muthu et al. (2008), Mandal (2005), Nasir and Alim (2017), Padmanabhan (1980)]. Most of these studies examined single-stenosis blood flow in a circular tube.

Akbar et al. (2014) have explored flow of Nanofluid in tapered stenosed arteries having permeable walls. Mekheimer and El Kot (2008) studied the blood flow model for the micropolar fluid through a tapered artery having single stenosis. The blood supply of fluids inside the stenosed arteries, critically analyzed by Akbar and Nadeem (2013). He (2000) and He (2005) explored the applications of Homotopy perturbation technique.

In this research investigation article, the proposed study of micropolar fluid flow in tapered artery having permeable walls is presented and explained the impact of different fluid flow parameters on flow impedance and shear stress.

2. Mathematical Formulation

A Cylindrical coordinate system (r, θ, z) with r=0 as axis of symmetry of the cylinder is considered such that z-axis is along the axis of artery. Consider an incompressible micropolar fluid over an inclined tapering artery having the stenosis with viscosity of fluid μ and density ρ.

The radial and circumferential direction be r and θ respectively The design of inclined stenosed tapered artery is given by Srivastava and Saxena (1997).

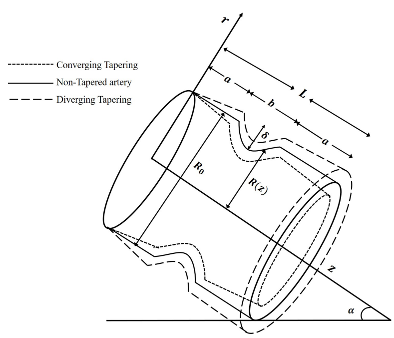

Figure 1: Geometry of Inclined Tapered stenosed artery

Assuming the stenoses are mild and create in axisymmetric way. The radius of the cylindrical shaped tube is

$$h = R(z) = \begin{cases} f(z) - \left[1 - \eta\left(b^{n-1}(z-a) - (z-a)^n\right)\right] & ; a \le z \le a+b \\ f(z) & ; \text{otherwise} \end{cases} \tag{1}$$

where $R(z)$ and R_0 are respectively the radius of tapered arterial segment in the stenotic and non-tapered arterial segment in the non-stenotic regions.

Here $f(z)=R_0+\xi z$, ξ denotes tapering parameter. b is the stenosis length, $n\geq 2$ is the shape parameter that determines stenosis shape. η is a parameter, given by $\eta = \frac{\delta}{R_0 b^n}\left(\frac{n^{\frac{1}{n-1}}}{n-1}\right)$, where δ is the maximum stenosis height at $z=a+\frac{b}{n^{\frac{1}{n-1}}}$.

The equations for the steady flow of micro polar fluid are (Mekheimer and El Kot (2008))

$$(\nabla\cdot W) = 0 \tag{2}$$

$$\rho(W\cdot\nabla W) = -(\nabla P) + (K\nabla\times W) + (\mu+K)\nabla^2 W \tag{3}$$

$$\rho j(W\cdot\nabla W) = -(2KV) + (K\nabla\times W) - \gamma(\nabla\times\nabla\times V) + (\alpha+\beta+\gamma)\nabla(\nabla\cdot V). \tag{4}$$

Here P is fluid pressure, j is microgyration parameter. K, μ are respectively the coefficients of vortex viscosities and shear stress. V and W are respectively the micro rotation and velocity vectors. α,β,γ are material constants satisfying inequalities given below

$$2\mu + K \geq 0, 3\alpha+\beta \geq 0, \gamma \geq |\beta|.$$

Thus, the equations for the fluid flow are

$$\frac{\partial w_r}{\partial r} + \frac{w_r}{r} + \frac{\partial w_z}{\partial z} = 0 \tag{5}$$

$$\rho\left(w_r\frac{\partial w_z}{\partial r} + w_z\frac{\partial w_z}{\partial z}\right) = -\frac{\partial P}{\partial z} + (\mu+K)\left(\frac{\partial^2 w_z}{\partial r^2} + \frac{1}{r}\frac{\partial w_z}{\partial r} + \frac{\partial^2 w_z}{\partial z^2}\right) + \frac{K}{r}\frac{\partial(rv_\theta)}{\partial r} \tag{6}$$

$$\rho\left(w_r\frac{\partial w_r}{\partial r} + w_z\frac{\partial w_r}{\partial z}\right) = -\frac{\partial P}{\partial r} + (\mu+K)\left(\frac{\partial^2 w_r}{\partial r^2} + \frac{1}{r}\frac{\partial w_r}{\partial r} - \frac{w_r}{r^2}\right) - K\frac{\partial v_\theta}{\partial z} \tag{7}$$

$$\rho j\left(w_r\frac{\partial v_\theta}{\partial r} + w_z\frac{\partial v_\theta}{\partial z}\right) = -2Kv_\theta - K\left(\frac{\partial w_z}{\partial r} - \frac{\partial w_r}{\partial z}\right) + \gamma\left(\frac{\partial}{\partial r}\left(\frac{1}{r}\frac{\partial(rv_\theta)}{\partial r}\right) + \frac{\partial^2 v_\theta}{\partial z^2}\right). \tag{8}$$

Here, $W=(w_r, 0, w_z)$ and $V=(0, v_\theta, 0)$ are respectively the velocity and micro-rotation vectors.

Introducing the non-dimensional variables

$$\bar{z}=\frac{z}{L},\ \bar{\delta}=\frac{\delta}{R_0},\ \bar{r}=\frac{r}{R_0},\ \bar{w_z}=\frac{w_z}{w_0},\ \bar{w_r}=\frac{Lw_r}{w_0\delta},\ \bar{w_\theta}=\frac{R_0 v_\theta}{w_0},\ \bar{J}=\frac{j}{R_0^2},\ \bar{p}=\frac{P}{\frac{\mu w_0 L}{R_0^2}}$$

into (5) - (8), the equations are:

$$\frac{\partial P}{\partial r} = -\frac{cos\alpha}{F} \tag{9}$$

$$\frac{N}{r}\frac{\partial}{\partial r}(rv_\theta)+\frac{\partial^2 w}{\partial r^2}+\frac{1}{r}\frac{\partial w}{\partial r}+(1-N)\frac{sin\alpha}{F}+(1-N)(G_r\theta_t+B_r\sigma)=(1-N)\frac{\partial P}{\partial z} \tag{10}$$

$$2v_\theta+\frac{\partial w}{\partial r}-\frac{2-N}{m^2}\frac{\partial}{\partial r}\left(\frac{1}{r}\frac{\partial}{\partial r}(rv_\theta)\right)=0 \tag{11}$$

$$\frac{1}{r}\frac{\partial}{\partial r}\left(r\frac{\partial \theta_t}{\partial r}\right)+N_b\frac{\partial \sigma}{\partial r}\frac{\partial \theta_t}{\partial r}+N_t\left(\frac{\partial \theta_t}{\partial r}\right)^2=0 \tag{12}$$

$$\frac{1}{r}\frac{\partial}{\partial r}\left(r\frac{\partial \sigma}{\partial r}\right)+\frac{N_t}{N_b}\left(\frac{1}{r}\frac{\partial}{\partial r}\left(r\frac{\partial \theta_t}{\partial r}\right)\right)=0. \tag{13}$$

Here $w{=}w_z$ is velocity in the axial direction, $N{=}\frac{k}{\mu+k}$; $(0\leq N<1)$, $m^2{=}\frac{R_0^2k(2\mu+k)}{\gamma(\mu+k)}$ (seeSrinivasacharya et al. (2003)), where N and m are respectively coupling number and micropolar parameter. θ_t, σ, N_t, N_b, B_r and G_r are temperature profile, nanoparticle phenomena, thermophoresis parameter, Brownian motion parameter, local nanoparticle Grashof number and local temperature Grashof number.

The non-dimensional boundary conditions are:

$$\left.\begin{array}{l}\frac{\partial w}{\partial r}=0\ ,\ \ \frac{\partial \theta_t}{\partial r}=0\ ,\ \ \frac{\partial \sigma}{\partial r}=0 \text{ at } r=0,\\ w=-k\frac{\partial w}{\partial r},\ \ \theta_t=0,\ \ \sigma=0 \text{ at } r=h\,(z)\,,\\ w \text{ is finite } \ \text{ at } r=0.\end{array}\right\} \tag{14}$$

3. Solution

The solutions of equations (12) and (13) are:

$$H(q_t,\theta_t)=(1-q_t)\left[L(\theta_t)-L(\theta_{10})\right]+q_t\left[L(\theta_t)+N_b\frac{\partial \sigma}{\partial r}\frac{\partial \theta_t}{\partial r}+N_t\left(\frac{\partial \theta_t}{\partial r}\right)^2\right], \tag{15}$$

$$H(q_t,\sigma)=(1-q_t)\left[L(\sigma)-L(\sigma_{10})\right]+q_t\left[L(\sigma)+\frac{N_t}{N_b}\left(\frac{1}{r}\frac{\partial}{\partial r}\left(r\frac{\partial \theta_t}{\partial r}\right)\right)\right], \tag{16}$$

where q_t is the embedding parameter $(0\leq q_t\leq 1)$. The linear operator is given by $L\equiv\frac{1}{r}\frac{\partial}{\partial r}\left(r\frac{\partial}{\partial r}\right)$.

θ_{10} and σ_{10} are the initial guesses given by:

$$\theta_{10}(r,z)=\left(\frac{r^2-h^2}{4}\right), \sigma_{10}(r,z)=-\left(\frac{r^2-h^2}{4}\right), \tag{17}$$

$$\theta_t(r,z)=\theta_{t_0}+q_t\theta_{t_1}+q_t^2\theta_{t_2}+\cdots, \tag{18}$$

$$\sigma(r,z)=\sigma_0+q_t\sigma_1+q_t^2\sigma_2+\cdots. \tag{19}$$

The series (18) and (19) are convergent in many cases. This convergent relies upon the non-linear part of the expression. For q_t=1, the solution for temperature profile (θ_t) and nanoparticle phenomena (σ) are:

$$\theta_t(r,z) = \left(\frac{r^2-h^2}{64}\right)(N_b - N_t), \tag{20}$$

$$\sigma(r,z) = -\left(\frac{r^2-h^2}{4}\right)\left(\frac{N_t}{N_b}\right). \tag{21}$$

By substituting the equations (20) and (21) in (10), the velocity equation is

$$\begin{aligned} w(r,z) = (1-N)\left(\frac{r^2-h^2}{4} - \frac{kr}{2}\right)\left(-\frac{sin\alpha}{F} + \frac{dP}{dz}\right) - N(r-h-k)v_\theta \\ + (1-N)B_r\left(\frac{N_t}{N_b}\right)\left(\frac{r^4}{64} - \frac{r^2h^2}{16} + \frac{3h^4}{64} - \frac{kr^3}{16} + \frac{krh^2}{8}\right) \\ - (1-N)G_r(N_b-N_t)\left(\frac{r^6}{2304} - \frac{r^2h^4}{256} + \frac{h^6}{288} - \frac{kr^5}{384} + \frac{krh^4}{128}\right). \end{aligned} \tag{22}$$

The dimension less flux (q) is

$$q = \int_0^h 2rwdr. \tag{23}$$

By substituting the equation (22) in (23), the flux is given by

$$\begin{aligned} q = (1-N)\left(\frac{h^4}{8} + \frac{kh^3}{3}\right)\left(\frac{sin\alpha}{F} - \frac{dP}{dz}\right) + N(h^3 + kh^2)v_\theta \\ + (1-N)B_r\left(\frac{N_t}{N_b}\right)\left(0.02083h^6 + 0.05833kh^5\right) - (1-N)G_r(N_b-N_t) \\ \left(0.001627h^8 + 0.004464kh^7\right). \end{aligned} \tag{24}$$

From the equation (24), $\frac{dP}{dz}$ can be obtained as

$$\begin{aligned} \frac{dP}{dz} = \frac{1}{\left(\frac{h^4}{8} + \frac{kh^3}{3}\right)}\Bigg[-\frac{q}{1-N} + \left(\frac{h^4}{8} + \frac{kh^3}{3}\right)\left(\frac{sin\alpha}{F}\right) + \\ \frac{N}{1-N}(h^3+kh^2)v_\theta - G_r(N_b-N_t)\left(0.001627h^8 + 0.004464kh^7\right) + \\ B_r\frac{N_t}{N_b}(0.02083h^6 + 0.05833kh^5)\Bigg]. \end{aligned} \tag{25}$$

The pressure drop per wave length Δp = $p(0)$ - $p(\lambda)$ is

$$\begin{aligned} \Delta p = -\int_0^1 \frac{dP}{dz}dz \\ \Rightarrow \Delta p = \int_0^1 \frac{1}{\left(\frac{h^4}{8} + \frac{kh^3}{3}\right)}\Bigg[\frac{q}{1-N} - \left(\frac{h^4}{8} + \frac{kh^3}{3}\right)\left(\frac{sin\alpha}{F}\right) - \\ \frac{N}{1-N}(h^3+kh^2)v_\theta + G_r(N_b-N_t)\left(0.001627h^8 + 0.004464kh^7\right) - \\ B_r\frac{N_t}{N_b}(0.02083h^6 + 0.05833kh^5)\Bigg]dz. \end{aligned} \tag{26}$$

The flow resistance (or) flow impedance (λ) is $\lambda = \frac{\Delta p}{q}$

$$\Rightarrow \lambda = \frac{1}{\left(\frac{h^4}{8} + \frac{kh^3}{3}\right)} \left[\frac{q}{1-N} - \left(\frac{h^4}{8} + \frac{kh^3}{3}\right)\left(\frac{sin\alpha}{F}\right) - \frac{N}{1-N}(h^3 + kh^2)v_\theta + G_r(N_b - N_t)\left(0.001627h^8 + 0.004464kh^7\right) - B_r\frac{N_t}{N_b}(0.02083h^6 + 0.05833kh^5)\right] dz. \quad (27)$$

Δp_n is pressure drop in the absence of stenosis ($h = 1$) and is attained from equation (26) as

$$\Delta p_n = \int_0^1 \frac{1}{\left(\frac{1}{8} + \frac{k}{3}\right)} \left[\frac{q}{1-N} - \left(\frac{1}{8} + \frac{k}{3}\right)\left(\frac{sin\alpha}{F}\right) - \frac{N}{1-N}(1+k)v_\theta + G_r(N_b - N_t)(0.001627 + 0.004464k) - B_r\frac{N_t}{N_b}(0.02083 + 0.05833k)\right] dz. \quad (28)$$

The flow impedance in the normal artery is (λ_n), given as

$$\lambda_n = \frac{\Delta p_n}{q}$$

$$= \frac{1}{q}\int_0^1 \frac{1}{\left(\frac{1}{8} + \frac{k}{3}\right)} \left[\frac{q}{1-N} - \left(\frac{1}{8} + \frac{k}{3}\right)\left(\frac{sin\alpha}{F}\right) - \frac{N}{1-N}(1+k)v_\theta + G_r(N_b - N_t)(0.001627 + 0.004464k) - B_r\frac{N_t}{N_b}(0.02083 + 0.05833k)\right] dz. \quad (29)$$

The normalized impedance to the flow is

$$\bar{\lambda} = \frac{\lambda}{\lambda_n}. \quad (30)$$

Wall shear stress is

$$\tau_h = -\frac{h}{2}\frac{dP}{dz} \quad (31)$$

$$= \frac{h}{2}\frac{1}{\left(\frac{h^4}{8} + \frac{kh^3}{3}\right)} \left[\frac{q}{1-N} - \left(\frac{h^4}{8} + \frac{kh^3}{3}\right)\left(\frac{sin\alpha}{F}\right) - \frac{N}{1-N}(h^3 + kh^2)v_\theta + G_r(N_b - N_t)\left(0.001627h^8 + 0.004464kh^7\right) - B_r\frac{N_t}{N_b}(0.02083h^6 + 0.05833h^5)\right]. \quad (32)$$

When $k = 0$, the equations are coincides with Mekheimer and El Kot (2008).

4. Results and Discussion

The equations (30) and (32) are equations for flow impedance ($\bar{\lambda}$) and shear stress (τ_h) respectively. Using Mathematica 9.1, the impact of different flow parameters on $\bar{\lambda}$ and τ_h with heights of stenosis were determined numerically.

To determine the impact of various parameters on $\bar{\lambda}$, the observations are noted for diverging tapering, non-tapered artery and converging tapering and are presented in Figures (2-9) for the values of local nanoparticle Grashof number (B_r), local temperature Grashof number (G_r), Thermophoresis parameter (N_t), Brownian motion number (N_b), Inclination (α), Shape parameter (n), Permeability constant (k) and Volumetric flow rate (q) under different shapes of stenosis.

It is seen that the $\bar{\lambda}$ increases with the increase of B_r, N_t, α and k and decreases with N_t, n and q. It is observed that, with the increase of local temperature Grashof number (G_r), the resistance to the flow is also increasing. But there is no much significance upto $\delta = 0.04$.

The impact of different fluid flow parameters on τ_h are shown in Figures (10-17). It is shown that, τ_h enhances with the increase of N_b and q, but decreases with B_r, G_r, N_t, n, k and α.

Streamlines: Figure(18) displays the streamlines for B_r. It is shown that, as we increase B_r, the bolus area is increasing and number of boluses are decreasing. Figure(19) reveals the behaviour of stream lines with heights of the stenosis (δ). It can be seen that the number of boluses is decreasing but the volume of bolus is slowly increasing. Figure(20) shows that more number of boluses are found with the increase of permeability constant (k), but bolus size is diminished.

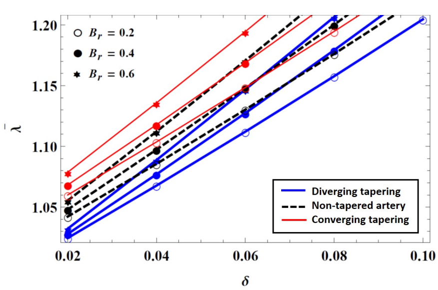

Figure 2: Effect of δ on $\bar{\lambda}$ with B_r varying

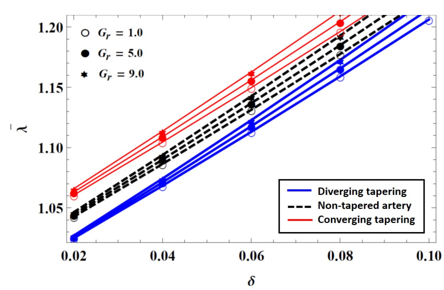

Figure 3: Effect of δ on $\bar{\lambda}$ with G_r varying

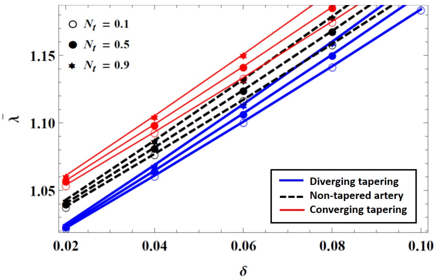

Figure 4: Effect of δ on $\bar{\lambda}$ with N_t varying

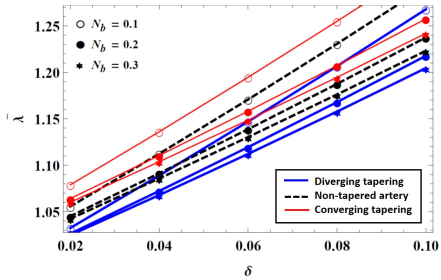

Figure 5: Effect of δ on $\bar{\lambda}$ with N_b varying

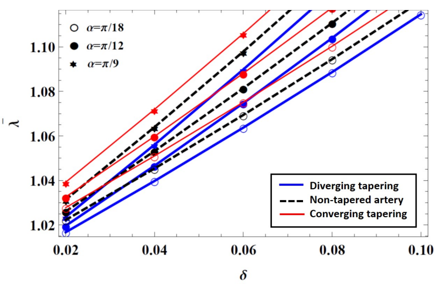

Figure 6: Effect of δ on $\bar{\lambda}$ with α varying

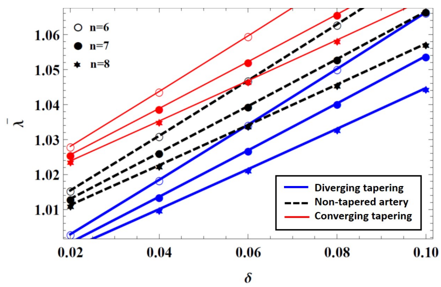

Figure 7: Effect of δ on $\bar{\lambda}$ with n varying

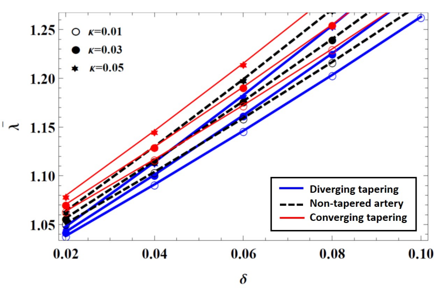

Figure 8: Variation of δ on $\bar{\lambda}$ with k varying

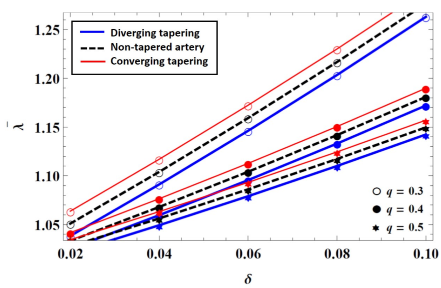

Figure 9: Variation of δ on $\bar{\lambda}$ with q varying

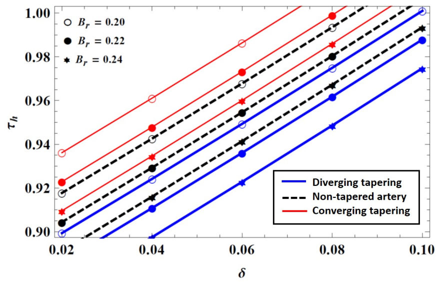

Figure 10: Variation of δ on τ_h with B_r varying

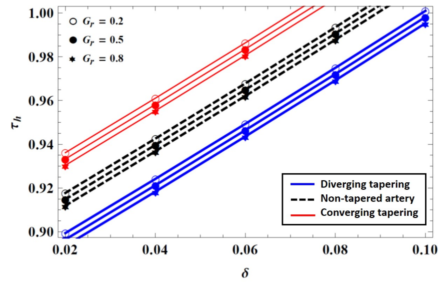

Figure 11: Variation of δ on τ_h with G_r varying

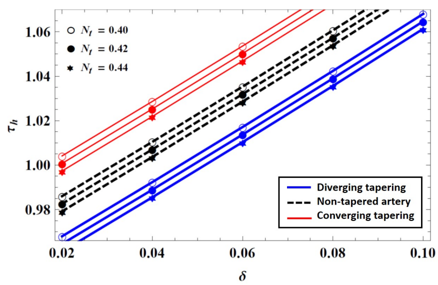

Figure 12: Variation of δ on τ_h with N_t varying

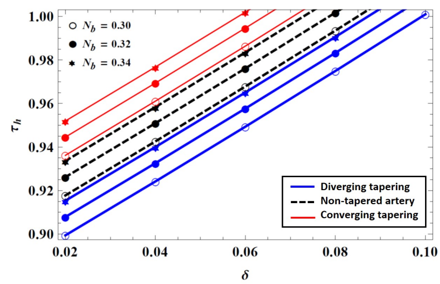

Figure 13: Variation of δ on τ_h with N_b varying

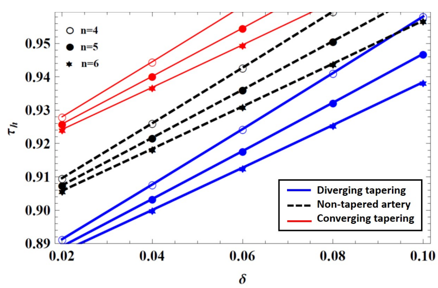

Figure 14: Variation of δ on τ_h with n varying

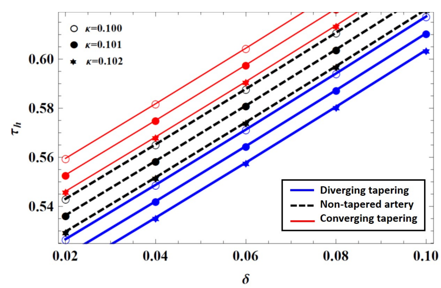

Figure 15: Variation of δ on τ_h with k varying

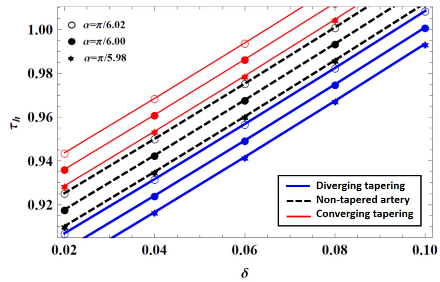

Figure 16: Variation of δ on τ_h with α varying

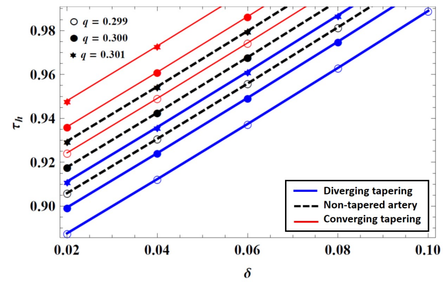

Figure 17: Variation of δ on τ_h with q varying

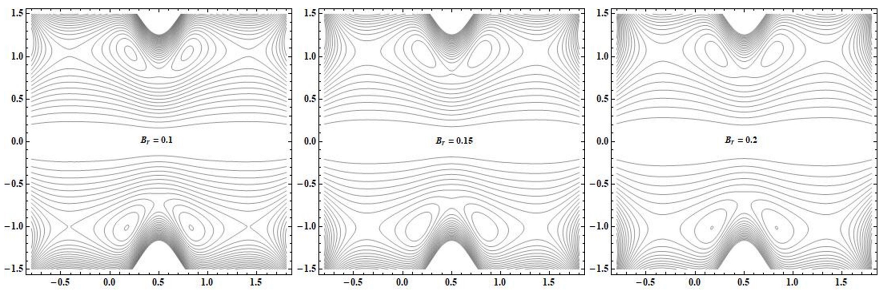

Figure 18: Streamlines for B_r=0.1, 0.15, 0.2

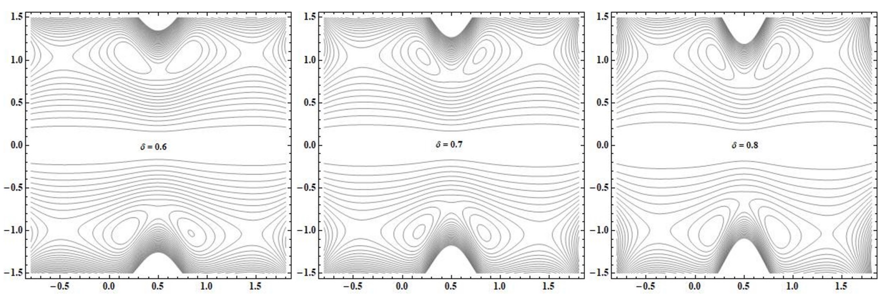

Figure 19: Streamlines for δ=0.6, 0.7, 0.8

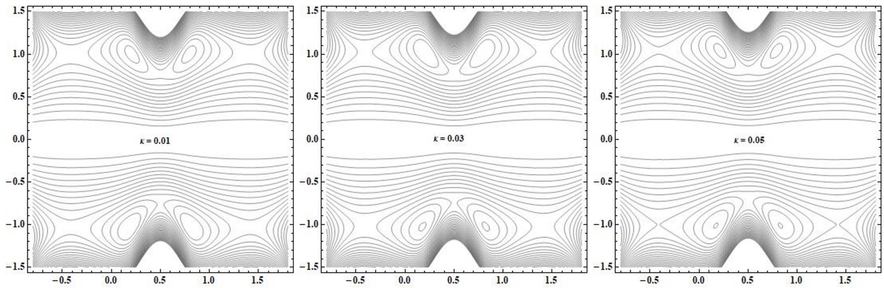

Figure 20: Streamlines for k=0.01, 0.03, 0.05

5. Conclusion

In this investigated research article, we presented micropolar fluid model in an inclined tapered stenosed artery having permeable walls. The inferences of this model are

1. The impedance to the flow is getting higher with B_r, α, k and getting lower with n for diverging tapering, non-tapered artery and converging tapering respectively.
2. It is interesting to note that, with the increase of G_r, the resistance to the flow is increasing with heights of the stenosis. But, this increase is significant only when the heights of the stenosis exceeds the value 0.04.
3. The velocity of the particles with the surrounding molecules (N_t) is noted increasing with the stenosis height.
4. It is important to note that, with the increase of collision between the molecules, the flow resistance decreases. i.e., Brownian motion parameter (N_b).
5. With the stenosis height expansion, the impact among the molecules rises with wall shear stress.
6. The shear stress at the wall drops with the increase of B_r, G_r, N_t, n, k and inclination (α).
7. More number of boluses are found with the increase of B_r, δ and k, but the bolus size is slowly decreasing.
8. In the absence of permeability constant (k), the results are coincides with Mekheimer and El Kot (2008).

Acknowledgement

We acknowledge and thank the reviewers for their valuable comments which help us to enrich the quality of this paper.

References

Abdullah, I. and Amin, N. (2010). A micropolar fluid model of blood flow through a tapered artery with a stenosis. *Mathematical Methods in the Applied Sciences*, 33(16):1910–1923.

Akbar, N. S. and Nadeem, S. (2013). Peristaltic flow of a micropolar fluid with nano particles in small intestine. *Applied Nanoscience*, 3(6):461–468.

Akbar, N. S., Rahman, S., Ellahi, R., and Nadeem, S. (2014). Nano fluid flow in tapering stenosed arteries with permeable walls. *International Journal of Thermal Sciences*, 85:54–61.

Eringen, A. C. (1966). Theory of micropolar fluids. *Journal of Mathematics and Mechanics*, 16(1):1–18.

Haghighi, A., Aliashrafi, N., and Kiyasatfar, M. (2019). Mathematical modeling of micropolar blood flow in a stenosed artery under the body acceleration and magnetic field. *International Journal of Industrial Mathematics*, 11(1):1–10.

He, J. (2000). Homotopy perturbation technique, computer methods in applied mechanics and engineering. *International Journal of Nonlinear Mechanics*, 35:37–43.

He, J.-H. (2005). Application of homotopy perturbation method to nonlinear wave equations. *Chaos, Solitons & Fractals*, 26(3):695–700.

Kumar, S. and Diwakar, C. (2013). Blood flow resistance for a small artery with the effect of multiple stenoses and post stenotic dilatation. *International Journal of Engineering Sciences & Emerging Technologies*, 6:57–64.

Mandal, P. K. (2005). An unsteady analysis of non-newtonian blood flow through tapered arteries with a stenosis. *International Journal of Non-Linear Mechanics*, 40(1):151–164.

Mekheimer, K. S. and El Kot, M. (2008). The micropolar fluid model for blood flow through a tapered artery with a stenosis. *Acta Mechanica Sinica*, 24(6):637–644.

Muthu, P., Kumar, B. R., and Chandra, P. (2008). Peristaltic motion of micropolar fluid in circular cylindrical tubes: Effect of wall properties. *Applied Mathematical Modelling*, 32(10):2019–2033.

Nasir, M. and Alim, M. (2017). Numerical study of blood flow through symmetry and non-symmetric stenosis artery under various flow rates. *IOSR Journal of Dental and Medical Sciences*, 16(6):106–115.

Padmanabhan, N. (1980). Mathematical model of arterial stenosis. *Medical and Biological Engineering and Computing*, 18(3):281–286.

Prasad, K. M., Radhakrishnamacharya, G., and Murthy, J. (2010). Peristaltic pumping of a micropolar fluid in an inclined tube. *International Journal of Applied Mathematics and Mechanics*, 6:26–40.

Prasad, K. M., Subadra, N., and Srinivas, M. (2015). Peristaltic transport of a nanofluid in an inclined tube. *American Journal of Computational and Applied Mathematics*, 5:117–128.

Prasad, K. M. and Yasa, P. R. (2020). Flow of non-newtonian fluid through a permeable artery having non-uniform cross section with multiple stenosis. *Journal of Naval Architecture and Marine Engineering*, 17(1):31–38.

Shukla, J., Parihar, R., and Rao, B. (1980). Effects of stenosis on non-newtonian flow of the blood in an artery. *Bulletin of Mathematical Biology*, 42(3):283–294.

Srinivasacharya, D., Mishra, M., and Rao, A. R. (2003). Peristaltic pumping of a micropolar fluid in a tube. *Acta Mechanica*, 161(3-4):165–178.

Srivastava, V. P. and Saxena, M. (1997). Suspension model for blood flow through stenotic arteries with a cell-free plasma layer. *Mathematical Biosciences*, 139(2):79–102.